ASSESSING THE PERFORMANCE OF OSCILLATING FIN THRUSTER VEHICLES

Mathieu Kemp, Brett Hobson, Jason Janét, Chuck Pell, Eric Tytell
Nekton Research, LLC
Durham, North Carolina
919-405-3993x275
fruitbat@nektonresearch.com

Abstract
In this article, we report on the performance of oscillating foil thrusters (OFT). Data from individual OFT performance as well as vehicle maneuvering performance suggest that future underwater vehicles may employ OFTs as control surfaces for vehicle orientation while cruising or as maneuvering thrusters while hovering. When operated in high impulsive force mode, the magnitude and response time of the thrust generated by OFTs could prove invaluable for emergency stopping or obstacle avoidance. As the control theory for this high impulsive thrust mode matures, OFTs may help future vehicles safely traverse the nearshore waters in higher sea states than is possible today.

1. Introduction

Many of today's small submersibles utilize control surfaces (dive planes and rudders) for orientation control while underway, but unless they are also equipped with vertical and lateral thrusters, hovering is not possible. It would be advantageous if these control surfaces could also be used as thrusters during docking or target classification maneuvers that require the ability to hover. Nekton Research has begun using modified control surfaces on one of its submersibles for three distinct uses: vehicle orientation control while cruising, vectored thrust for hovering, and high impulse force generation for collision avoidance and high energy station keeping.

Near shore, and especially in the surf zone, waves and other currents cause high transient accelerations. The AUVs in use today are designed for use in calm seas. They are therefore unable to compensate for the high transient accelerations experienced in the near shore region. These vehicles use propellers for forward thrust and dive planes or outboard thrusters for orientation control. Because propellers must build circulation to produce thrust, the response tends to lag behind the request. The lag is particularly problematic in reversing flows where the propeller must rapidly change direction. The consequence of lagging or insufficient thrust while operating an AUV in shallow water is imminent impact with the seafloor. If an AUV must enter the nearshore region to search for mines, a means of rapidly generating very large forces and a crash resistant design will be needed.

Nekton's OFT (Nektor, Figure 1) consists of a flexible fin mounted on a rotary actuator about its quarter chord. Nektors are strictly pitching OFTs, in contrast to other OFTs that pitch and/or heave [1-8]. Nektors have two modes of thrust production, continuous and high impulse (Figure 2). Oscillating the fin produces a lift-based, continuous rearward jet (reversed Karman street) that can be

vectored around the actuator shaft. Alternatively, the actuator can be programmed for quick, large amplitude motion between two orientations, producing a sudden burst of thrust.

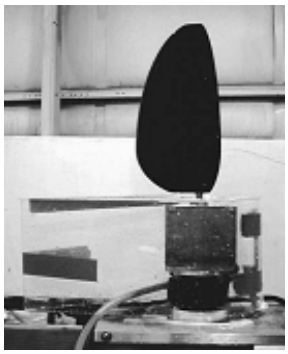

Figure 1: Oscillating fin thruster (OFT) mounted on a 6-axis load cell.

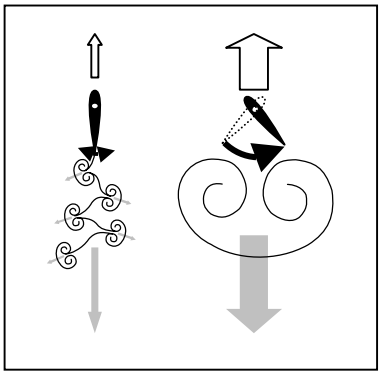

Figure 2: two modes of thrust production. Left: continuous. Right: high impulse.

This paper is organized as follows. In Section 2 we present time-resolved data for the performance of individual OFTs. In Section 3, we present data on the maneuvering performance of a UUV fitted with OFTs. In Section 4 we discuss future work.

2. Oscillating Fin Thruster Characterization

We performed experiments aimed at characterizing the continuous mode of thrust production. The experiments were carried out at Florida Atlantic University's flow tank (1.2m x 1.2m working section @ 0-1 knot). Two fins of different stiffness were used (NACA profile 0014, rectangular planform, Shore A 25 and 70 polyurethane, chord 11.5cm, span 15cm). The fins are mounted on a 2.5kW direct-drive servomotor (Kollmorgen DC brushless motor). A DeltaTau board controls OFT motion. Loads are measured with a six-axis load cell (JR3 100M40A, 0.1N resolution). Data collection (6-axis loads, motor current, and fin location) is done at 20hz from a Matlab interface.

In continuous mode, the OFT profile is

$$\theta(t) = \theta_c + \Delta\cos(\omega t + \varphi), \qquad \text{(Eq. 1)}$$

where $\theta(t)$ is the location of the fin at time t, θ_c is the center of oscillation, Δ is the amplitude, ω is the frequency, and φ is a phase factor. We set $\theta_c=\varphi=0$, and vary the frequency (2-6hz) and amplitude of oscillation (10-30º). Data is collected for 30 seconds at each frequency/amplitude combination.

Although six axes of load data are collected, only three are relevant: force along the center of oscillation (thrust axis), force perpendicular to it (lateral axis), and axial torque.

Figure 3 shows the time-resolved thrust and lateral forces on the stiff fin during an oscillation. The frequency is 3.4hz and the amplitude is 30º. The force along the lateral axis is symmetrical around the halfway point and around zero. Its maximum is 30N. Superimposed over the 3.4hz signal is a 50hz oscillation. This oscillation is not a result of noise, as we observed it throughout the 100 oscillations over which the data was collected. The pattern of force along the thrust axis repeats itself during the first and second halves of the cycle. Over each

half cycle, thrust rises to 20N then decreases to –5N.

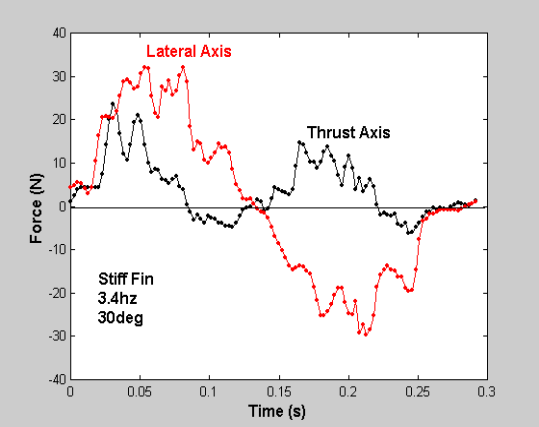

Figure 3: Time-resolved loads along the thrust and lateral axes.

A simple explanation is as follows. The fin acts as a drag plane. When its speed relative to the fluid increases, drag increases. Because drag is applied normal to the plane of the fin, the lateral force is symmetrical around the halfway point of the trajectory and around zero force. Hence, the net lateral force over a cycle is zero. By the same argument, net thrust should be zero in each half cycle, however when the fin moves, it entrains the fluid in its direction, so that when the motion reverses, the drag on the fin is momentarily higher. For this reason, thrust does not average to zero.

We are currently not able to explain the high-frequency component of the signal, though potential candidate explanations include periodic vortex shedding, membrane oscillations, and shaft oscillations. We find that both the frequency and amplitude of the high-frequency component increase as the baseline frequency increases (30hz at baseline=2.4hz to 80hz at baseline=6.4hz, Figure 4). We also find that the high-frequency component varies little as the baseline amplitude of oscillation changes, and that they are weakly dependent on fin stiffness.

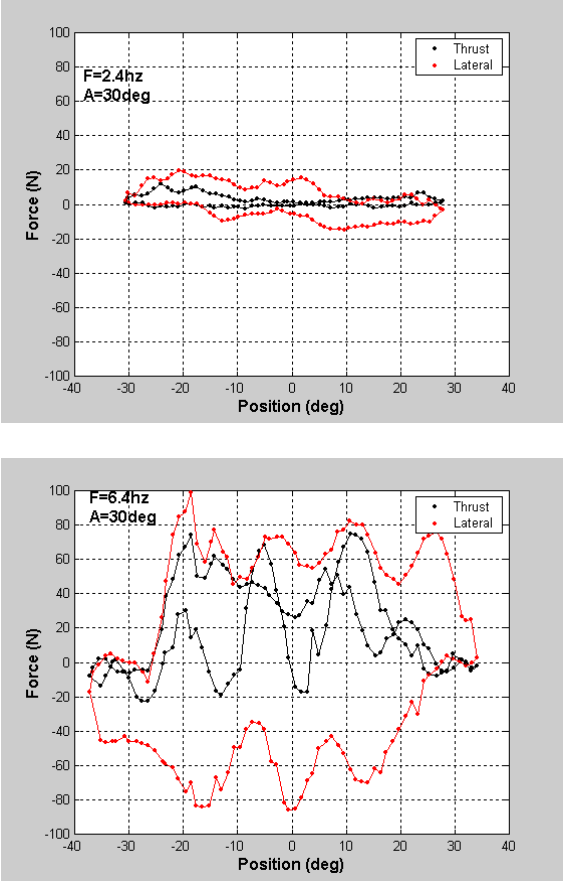

Figure 4: Loads along the thrust and lateral axes as a function of fin position. Top: stiff fin at 2.4hz. Bottom: stiff fin at 6.4hz.

Figure 5 shows the dependence of net thrust on frequency and amplitude. Net thrust is defined as

$$< \text{Thrust} >= \frac{1}{T}\int_0^T \text{Thrust}(t)dt \,. \qquad \text{(Eq. 2)}$$

We find that net thrust is a simple function of the product frequency times amplitude, $<\text{Thrust}> \sim (f\Delta)^{1.9+/-0.2}$. We also find that the stiff fin produces ~20% more thrust than the soft one.

The figure of merit for low speed maneuvers is the Bollard efficiency. The Bollard efficiency is equal to the ratio of actual thrust over the thrust that would be

produced by an ideal actuator disk of the same area with the same power:

$$\eta = \frac{< \text{Thrust} >}{\left(2\rho A P^2\right)^{2/3}}, \qquad \text{(Eq. 3)}$$

where A is the propeller area and P the power. For a Nektor, the relevant area is the rectangular arc traced by the fin trailing edge (2×amplitude in radians×chord×span), and power is found by integrating the product of axial torque and angular velocity:

$$P = \frac{\int_0^T dt\, \text{Torque}(t) * d\theta/dt}{T} \qquad \text{(Eq. 4)}$$

The efficiency is shown in Figure 6. For large values of fΔ, η is constant at 0.4. For smaller values, the efficiency increases as fΔ decreases. The soft fin is slightly more efficient than the stiff one.

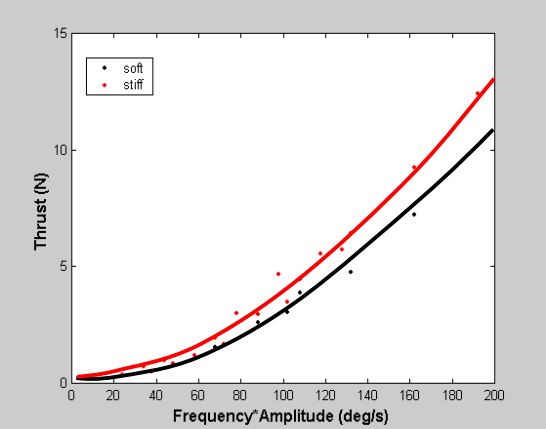

Figure 5: net thrust as a function of fΔ product for the stiff and soft fins.

In comparison, propellers of comparable area have an efficiency of ~0.7. Large propellers fall in the range η~1.2-1.8. Compared with props of the same size, Nektors have half the efficiency, which is encouraging because it was achieved without fin optimization. Fin optimization is currently underway, and results will be presented as they become available.

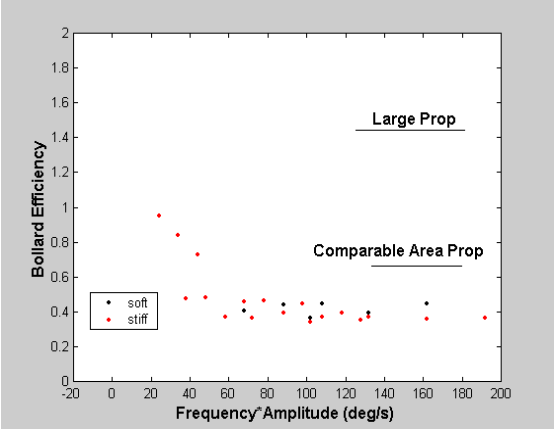

Figure 6: Bollard efficiency as a function of fΔ.

3. PilotFish Performance

3.1. Vehicle Description

We have previously discussed the design of PilotFish, a vehicle aimed at demonstrating the capabilities of Nektors [4]. PilotFish is a 150kg, 50cm diameter, rigid hull UUV, with four Nektors in a transverse-X configuration, driven by four 2.5kW direct-drive servomotors (Figure 7). Power is provided by a 1.4kWh lead-acid battery pack capable of providing short-duration, high-current loads, typical of high-impulse thrust propulsion. The fins are made of Shore A 60 polyurethane (NACA 0010 profile with elliptical planform, chord=20cm, span=40cm). The motor controller records the position of individual Nektors at 86Hz. A Crossbow DMU-VGX measures vehicle acceleration at 140Hz with a precision of ±0.006*g*.

3.2. Control

As discussed previously, OFTs have two modes of thrust production, continuous and high impulse. Oscillating the fin produces a continuous rearward jet (reversed Karman street) that can be steered in any direction around the actuator shaft. As discussed in Section 2, this produces moderate amounts of thrust, comparable with that generated by

propellers. Alternatively, the actuator can be programmed for quick, large amplitude motion between two orientations to produce sudden bursts of thrust. Multiple Nektors on a single vehicle can operate in either mode, independent of each other.

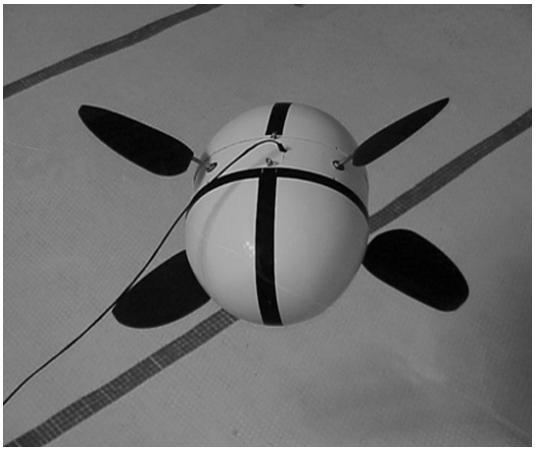

Figure 7: PilotFish.

From the control standpoint, these modes are very different. In *continuous mode*, Nektors are best thought of as low thrust, variable output, omni-directional thrusters. From the time-resolved data of Section 2, thrust is produced in high frequency bursts (>20hz), however the inertia of the vehicle filters out most of it, leaving only the DC component. Writing the force and torque equations along the three body axes:

$$\begin{bmatrix} F_x \\ \tau_2/a \\ \tau_3/a \end{bmatrix} = M \begin{bmatrix} f_1^x \\ f_2^x \\ f_3^x \\ f_4^x \end{bmatrix}; \begin{bmatrix} -\tau_1/2ab \\ F_y/b \\ F_z/b \end{bmatrix} = M \begin{bmatrix} f_1^z \\ f_2^z \\ f_3^z \\ f_4^z \end{bmatrix}$$

$$M = \begin{bmatrix} 1 & 1 & 1 & 1 \\ 1 & -1 & -1 & 1 \\ -1 & -1 & 1 & 1 \end{bmatrix}; \qquad \text{(Eq.5)}$$

$$f_i^x = |f_i| \cos\theta_i ; f_i^z = |f_i| \sin\theta_i$$

where a is the moment arm divided by $\sqrt{2}$, and $b=1/\sqrt{2}$, we find that the matrix M has three non-zero singular values, proving that PilotFish is controllable.

In contrast to the continuous mode, a theory of control in *high impulse mode* still awaits. The main obstacle is the construction of an OFT plant. Unsteady solid-fluid interactions are essential in this mode, and unsteady dynamics are difficult to model without the introduction of a large number of fluid degrees of freedom. Neglecting unsteady effects, i.e. treating each fin as a drag plane, net thrust should be directed parallel to the mid-point of the high-amplitude motion, and thrust magnitude should be proportional to $(\Delta\theta/T)^2$, where $\Delta\theta$ is the amplitude of motion and T is the impulse time. As we will show below, this is sufficient to provide reasonable control of the vehicle.

Relative phasing of the fins is important (Equation 2). We have identified three dominant phase regimes: equal, even, and odd. 'Equal' phase is when the fins oscillate in phase with each other: $\varphi_1=\varphi_2=\varphi_3=\varphi_4=0$. 'Even' is when the fins diagonally across from each other are in phase, and the other two 180° out of phase: $\varphi_1=\varphi_3=0$, $\varphi_2=\varphi_4=\pi$. 'Odd' phase is when the motors horizontally across from each other are in phase and the upper and lower pairs are 180° out of phase: $\varphi_1=\varphi_4=0$, $\varphi_2=\varphi_3=\pi$.

3.3. Continuous Mode

We investigated the continuous mode of thrust production by recording the acceleration on the body during translation along the forward axis. The fins were oscillated at 2hz. For even phasing, we recorded 0.1*g* acceleration spikes every half period, just before the trailing edge of each fin crosses the forward axis (Figure 8). This is consistent with the data in Figure 4. Lateral and

vertical motions are small. Odd phasing produces smaller spikes (0.06*g*) and larger lateral motion (Figure 9). Equal phasing generates slightly less forward movement and a larger unwanted rolling motion. Despite the fact that equal phasing is effective for flips, it is the least effective pattern for low amplitude motion.

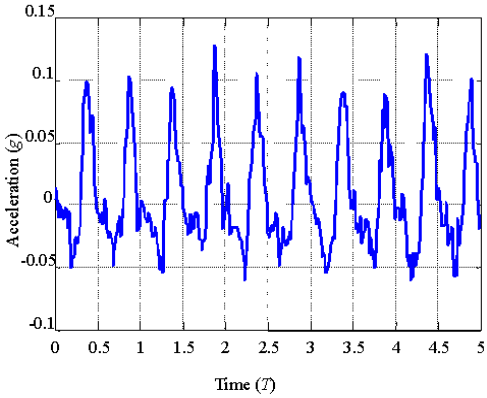

Figure 8: Vehicle acceleration in the forward direction for even phasing. Time is normalized by the oscillation period.

We believe that the effectiveness of even phasing is a result of the opposed motion of the fins. When two trailing edges come together, they appear to produce a larger force. This may be a result of interaction between the shed vorticity from each fin when the trailing edges are close together. Thus, even phasing produces little lateral motion, because each time the trailing edges come together, the left and right, or dorsal and ventral sides oppose each other.

3.4. High Impulse Mode

To examine the high impulse mode, we used two Nektor flip amplitudes, 90° and 180°. The largest accelerations are seen during the 90° flips. The fins first move from a downward to a backward configuration, then switch to continuous thrust mode. The flip takes 180ms.

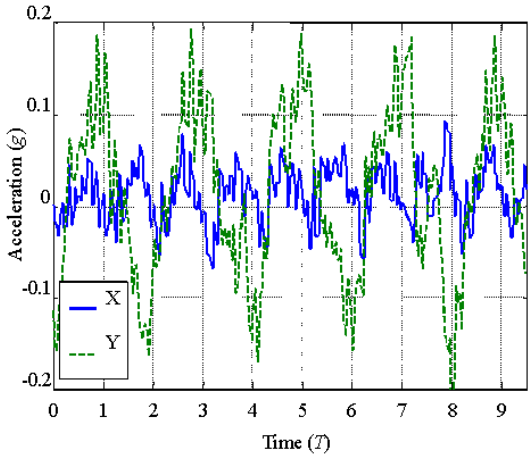

Figure 9: Vehicle acceleration in the forward (X) and lateral (Y) directions for odd phasing.

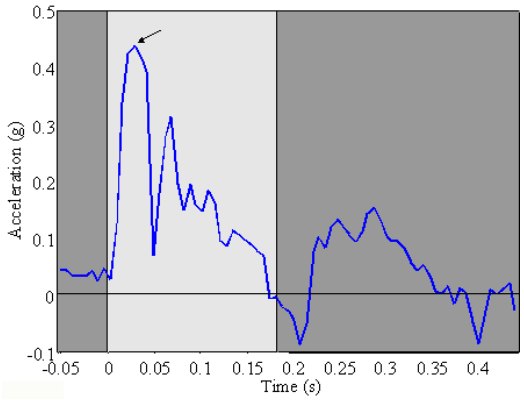

Figure 10: thrust development during and after a 90° flip. Light:flip. Dark: low amplitude oscillations.

Figure 10 shows that the acceleration of the vehicle rises to 0.4*g* in 20-30ms, and reaches 0 at the end of the flip.

Figure 11 below shows the result of applying a 180° flip. The fins are initially positioned facing forward. Flip time is 300ms. Even and odd phasings generate similar forward accelerations (0.2g). Odd phasing produces large upward accelerations (0.2g), while even phasing produces small lateral and upward accelerations but large oscillations. Odd and even phasing create small pitching and rolling moments. Equal phasing produces the largest accelerations, both forward (0.35*g*) and laterally (0.27*g*), with

little upward motion; it also produces large rolling motions (130 deg s^{-1}).

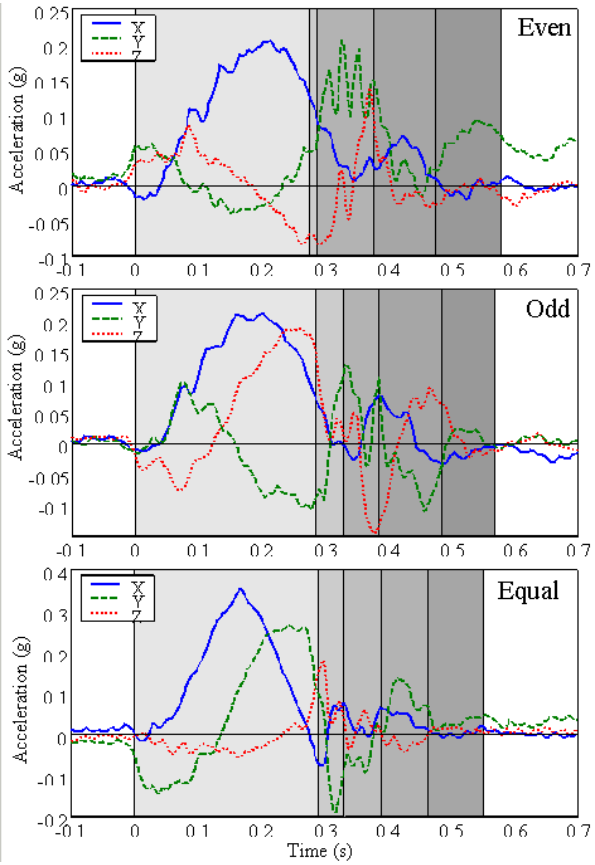

Figure 11: Acceleration during 180° flips.

Given the magnitude of the forces that are being generated, the stopping distance is expected to be small. We have found that PilotFish (157kg) can stop from a forward velocity of 0.6ms^{-1} over a distance of 12cm. This is consistent with the accelerations reported above (sinusoidal profile for 0.3s over 180°, drag coefficient of 1, fin speed measured at 10cm from shaft).

3.5. Discussion

The continuous mode of thrust production is appropriate to situations where fine control is needed, for example hovering and roll/pitch compensation. In contrast, the high-impulse mode is appropriate for sudden, high-impulse maneuvers. A feature that is specific to OFTs, which remains to be addressed, is that of efficient reorientation of the fins. In high-energy maneuvers, disturbances are unpredictable, strong, and omni-directional. Thrust application must therefore be swift, variable, and steerable. Speed and magnitude of the response is controlled by the duration and amplitude of the OFT flip. Efficient means of controlling the orientation are still being sought. The main obstacle to implementing steerability is that the orientation of each fin must be initialized before the start of the flip, else thrust is not produced in the right direction. During initialization, the OFTs produce parasitic forces whose magnitude depends on the speed and amplitude of the reorientation. Thus, a compromise between speed of reorientation and magnitude of the parasitic forces must be struck. We believe that concerted motion strategies exist that can reduce the magnitude of parasitic forces. A mechanism is also being explored that will allow the fin to fold or feather during initialization, then release into a locked position during the thrust stroke. Since one of the strengths of the OFTs is mechanical simplicity, we favor a control scheme over an increase in mechanical complexity.

4. Future Work

A retrofit Nektor module is currently (Summer 2001) being built for the Morpheus AUV developed at Florida Atlantic University [11]. The modular design of Morpheus allows accessory modules to be added or removed for different missions, and is an ideal platform to introduce OFTs as a commercial product. The self-contained Nektor module being built by Nekton Research receives upper level control requests (e.g. thrust/torque vector and

magnitude) from the centralized navigation computer via a TCP/IP network while power (nominal 60 Vdc) is pulled from Morpheus' main battery pack. Four, 157-watt motors, their amplifiers, controllers, power supplies and associated hardware have been squeezed into a single module. An alternative, thruster-based hovering option exists, though two separate modules are required. Using the fairly well understood, continuous thrust mode described above, this hovering module will enable Morpheus to perform complex docking or target classification maneuvers. In addition to slow hovering, obstacle avoidance maneuvers like the emergency stop performed by Pilotfish (157kg vehicle can stop from 0.6ms^{-1} over a distance of 12cm) will be possible. As we gain a better understanding of the Nektor's high impulse mode of thrust production, we hope to begin operating Morpheus in higher sea states than attempted so far. Alternative vehicle platforms that may be candidates for future OFT conversion are the Naval Post Graduate School's Aries AUV and Sias/Patterson's Fetch2. Certainly, the designers of the next generation of shallow water, mine hunting AUVs should consider utilizing OFTs.

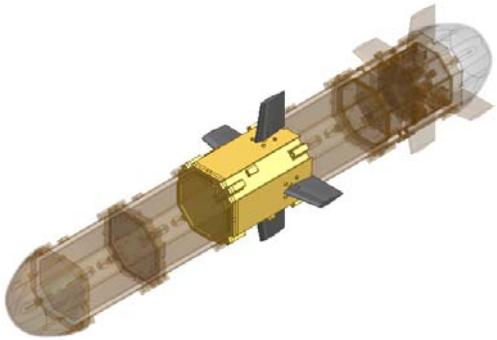

Figure 12: OFT module fitted amidships on the Morpheus AUV

5. Summary

We have examined the performance of oscillating fin thrusters, both on individual thrusters and on a vehicle. OFTs can operate in two modes of thrust production: high impulse and continuous. In continuous mode, we find that thrust is a simple function of the frequency/amplitude product. We also find that the Bollard efficiency is half that of propellers, however this figure is expected to improve with fin optimization. From a control standpoint, this mode is well enough characterized to be portable to other vehicles. In high impulse mode, the forces produced by OFTs are large. Although symmetry arguments can be used that make it possible to construct approximate control schemes, a solid control theory still awaits. This aspect is currently being examined through an ONR-sponsored joint effort between Nekton Research and Florida Atlantic University.

Acknowledgments

This work was performed under ONR support through grants N00014-97-C-0462 and N00014-C-00-0445. We thank Duke University for access to their deep diving pool, and Florida Atlantic University for access to their flow tank. We thank Eric Tytell for his work on vehicle characterization. We thank Chris Mailey for setting up the data acquisition interface and Jeff Goldman for setting up the fin characterization experiment. We also thank Chuck Pell, Laurens Howle, Steve Katz, William Vorus, and Alexander Leonessa for numerous discussions, assistance, and insight.

References

[1] Triantafyllou, G. S., Triantafyllou, M. S., and Grosenbaugh, M. A. (1993). "Optimal thrust development in

oscillating foils with application to fish propulsion." *J.Fluids Struct.* **7**: 205-224.

[2] Saimek, S., and Li, P.Y., (2001). "Motion Planning and control of a Swimming Machine." *Proc. Am. Control Conf.*: 125.

[3] Streitlien, K., "A Simulation Procedure for Vortex Flow Over an Oscilating Wing", *MIT SeaGrant Report MITSG 94-7*.

[4] Hobson, B., Murray, M., and Pell, C. A. (1999). "PilotFish: Maximizing agility in an unmanned-underwater vehicle." *Int.Symp.Unmanned Untethered Submersible Tech.* **11**: 41-51.

[5] Pell, C. A. and Wainwright, S. (1997). "Development and testing of a highly maneuverable underwater vehicle: Prototype platform maneuvered by Nektor thrusters." *ONR STTR N00014-96-C-0319*.

[6] Pell, C. A. *et al.* (1997). "Development and testing of flexible, high-maneuverability propulsion nacelles." *ONR STTR N00014-96-C-0319*.

[7] Wainwright, S., Pell, C. A., and Keller, I. (1997). "A fishlike, flexible thruster: Assessment of radiated noise and propulsion performance." *ONR STTR N00014-96-C-0008*.

[8] Anderson, J. M. and Kerrebrock, P. A. (1999). "The vorticity control unmanned undersea vehicle (VCUUV) performance results." *Int.Symp.Unmanned Untethered Submersible Tech.* **11**: 360-369.

[9] Bachmayer, R. *et al.* (1997). "Unsteady three-axis force, torque and flow dynamical modeling and experiments with marine thrusters." *Int.Symp.Unmanned Untethered Submersible Tech.* **10**: 1-8.

[10] Bachmayer, R., Whitcomb, L., and Grosenbaugh, M. A. (2000). "An accurate four-quadrant nonlinear dynamical model for marine thrusters: Theory and experimental validation." *IEEE J.Oceanic Eng.* **25**: 146-159.

[11] S. Smith et. Al., (1999), "An Ultra Modular Plastic Mini AUIV Platform for VSW Mine Reconnaissance, *Proceedings of Spie*.